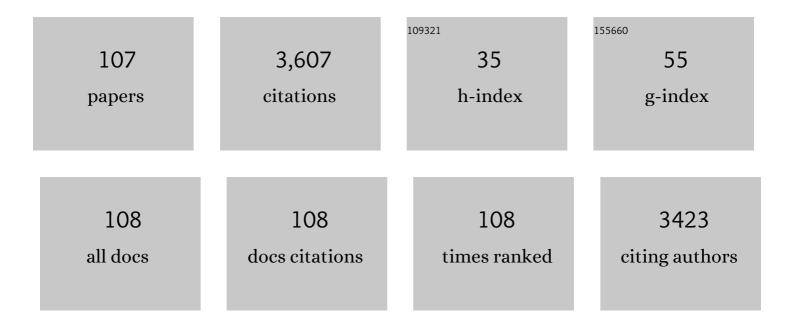
Shule Zhang

List of Publications by Year in descending order

Source: https://exaly.com/author-pdf/8231864/publications.pdf Version: 2024-02-01



#	Article	IF	CITATIONS
1	Hierarchical Z-scheme photocatalyst of g-C3N4@Ag/BiVO4 (040) with enhanced visible-light-induced photocatalytic oxidation performance. Applied Catalysis B: Environmental, 2018, 221, 97-107.	20.2	303
2	Simultaneous removal of NOX and SO2 from coal-fired flue gas by catalytic oxidation-removal process with H2O2. Chemical Engineering Journal, 2014, 243, 176-182.	12.7	163
3	Promotional effect of F-doped V2O5–WO3/TiO2 catalyst for NH3-SCR of NO at low-temperature. Applied Catalysis A: General, 2012, 435-436, 156-162.	4.3	125
4	Amino-Assisted NH ₂ -UiO-66 Anchored on Porous g-C ₃ N ₄ for Enhanced Visible-Light-Driven CO ₂ Reduction. ACS Applied Materials & Interfaces, 2019, 11, 30673-30681.	8.0	116
5	Ultrasound assisted synthesis of heterogeneous g-C3N4/BiVO4 composites and their visible-light-induced photocatalytic oxidation of NO in gas phase. Journal of Alloys and Compounds, 2015, 626, 401-409.	5.5	106
6	Single Pt atoms deposition on g-C3N4 nanosheets for photocatalytic H2 evolution or NO oxidation under visible light. International Journal of Hydrogen Energy, 2017, 42, 27043-27054.	7.1	97
7	Construction of Z-scheme photocatalytic systems using ZnIn 2 S 4 , CoO x -loaded Bi 2 MoO 6 and reduced graphene oxide electron mediator and its efficient nonsacrificial water splitting under visible light. Chemical Engineering Journal, 2017, 325, 690-699.	12.7	94
8	Promotional effect of WO3 on O2â^' over V2O5/TiO2 catalyst for selective catalytic reduction of NO with NH3. Journal of Molecular Catalysis A, 2013, 373, 108-113.	4.8	89
9	Sol–gel synthesis of CuO-TiO 2 catalyst with high dispersion CuO species for selective catalytic oxidation of NO. Applied Surface Science, 2017, 411, 227-234.	6.1	79
10	Efficient visible-light photocatalytic oxidation of gaseous NO with graphitic carbon nitride (g–C3N4) activated by the alkaline hydrothermal treatment and mechanism analysis. Journal of Hazardous Materials, 2015, 300, 598-606.	12.4	76
11	A New Insight into Catalytic Ozonation with Nanosized Ce–Ti Oxides for NO _{<i>x</i>} Removal: Confirmation of Ce–O–Ti for Active Sites. Industrial & Engineering Chemistry Research, 2015, 54, 2012-2022.	3.7	74
12	Synergistic degradation mechanism of chlorobenzene and NO over the multi-active center catalyst: The role of NO2, BrÃ,nsted acidic site, oxygen vacancy. Applied Catalysis B: Environmental, 2021, 286, 119865.	20.2	70
13	CeO2 supported on reduced TiO2 for selective catalytic reduction of NO by NH3. Journal of Colloid and Interface Science, 2017, 496, 487-495.	9.4	69
14	Graphene-decorated 3D BiVO4 superstructure: Highly reactive (040) facets formation and enhanced visible-light-induced photocatalytic oxidation of NO in gas phase. Applied Catalysis B: Environmental, 2016, 193, 160-169.	20.2	64
15	Enhanced catalytic ozonation for NOx removal with CuFe 2 O 4 nanoparticles and mechanism analysis. Journal of Molecular Catalysis A, 2016, 424, 153-161.	4.8	63
16	Surface characterization studies on the interaction of V2O5–WO3/TiO2 catalyst for low temperature SCR of NO with NH3. Journal of Solid State Chemistry, 2015, 221, 49-56.	2.9	62
17	Effect of Y doping on oxygen vacancies of TiO2 supported MnOX for selective catalytic reduction of NO with NH3 at low temperature. Catalysis Communications, 2012, 25, 7-11.	3.3	60
18	Catalytic efficiency of iron oxides in decomposition of H2O2 for simultaneous NOX and SO2 removal: Effect of calcination temperature. Journal of Molecular Catalysis A, 2014, 393, 222-231.	4.8	59

#	Article	IF	CITATIONS
19	Simultaneous removal of NOX and SO2 with H2O2 over Fe based catalysts at low temperature. RSC Advances, 2014, 4, 5394.	3.6	53
20	The effect of CuO loading on different method prepared CeO2 catalyst for toluene oxidation. Science of the Total Environment, 2020, 712, 135635.	8.0	52
21	One-step hydrothermal synthesis of a novel 3D BiFeWO _x /Bi ₂ WO ₆ composite with superior visible-light photocatalytic activity. Green Chemistry, 2018, 20, 3014-3023.	9.0	51
22	Effects of synthesis methods on catalytic activities of CoO x –TiO 2 for low-temperature NH 3 -SCR of NO. Journal of Environmental Sciences, 2017, 54, 277-287.	6.1	50
23	Novel Fe-doped CePO4 catalyst for selective catalytic reduction of NO with NH3: The role of Fe3+ ions. Journal of Hazardous Materials, 2020, 383, 121212.	12.4	50
24	Supramolecular Synthesis of Multifunctional Holey Carbon Nitride Nanosheet with Highâ€Efficiency Photocatalytic Performance. Advanced Optical Materials, 2017, 5, 1700536.	7.3	49
25	Simultaneous desulfurization and denitrification of flue gas by catalytic ozonation over Ce–Ti catalyst. Fuel Processing Technology, 2014, 128, 449-455.	7.2	46
26	Surface characterization studies on F-doped V2O5/TiO2 catalyst for NO reduction with NH3 at low-temperature. Chemical Engineering Journal, 2014, 253, 207-216.	12.7	45
27	One-pot synthesis of ceria and cerium phosphate (CeO2-CePO4) nanorod composites for selective catalytic reduction of NO with NH3: Active sites and reaction mechanism. Journal of Colloid and Interface Science, 2018, 524, 8-15.	9.4	45
28	<i>In situ</i> self-assembly of zirconium metal–organic frameworks onto ultrathin carbon nitride for enhanced visible light-driven conversion of CO ₂ to CO. Journal of Materials Chemistry A, 2020, 8, 6034-6040.	10.3	45
29	In-situ growth UiO-66-NH2 on the Bi2WO6 to fabrication Z-scheme heterojunction with enhanced visible-light driven photocatalytic degradation performance. Colloids and Surfaces A: Physicochemical and Engineering Aspects, 2020, 603, 125256.	4.7	43
30	Size- and shape-controlled synthesis and catalytic performance of iron–aluminum mixed oxide nanoparticles for NOX and SO2 removal with hydrogen peroxide. Journal of Hazardous Materials, 2015, 283, 633-642.	12.4	42
31	New insight into the promoting role of process on the CeO2–WO3/TiO2 catalyst for NO reduction with NH3 at low-temperature. Journal of Colloid and Interface Science, 2015, 448, 417-426.	9.4	40
32	Enhanced NOx removal performance of amorphous Ce-Ti catalyst by hydrogen pretreatment. Journal of Molecular Catalysis A, 2016, 423, 371-378.	4.8	40
33	A study on the NH ₃ -SCR performance and reaction mechanism of a cost-effective and environment-friendly black TiO ₂ catalyst. Physical Chemistry Chemical Physics, 2018, 20, 22744-22752.	2.8	39
34	Protonic acid-assisted universal synthesis of defect abundant multifunction carbon nitride semiconductor for highly-efficient visible light photocatalytic applications. Applied Catalysis B: Environmental, 2019, 258, 118011.	20.2	38
35	Recent Progress of CeO ₂ â ^{~>} TiO ₂ Based Catalysts for Selective Catalytic Reduction of NO _x by NH ₃ . ChemCatChem, 2021, 13, 491-505.	3.7	38
36	Structural characterizations of fluoride doped CeTi nanoparticles and its differently promotional mechanisms on ozonation for low-temperature removal of NO x (x = 1, 2). Chemical Engineering Journal, 2016, 286, 549-559.	12.7	36

#	Article	IF	CITATIONS
37	Synthesis and characterization of direct Z-scheme Bi2MoO6/ZnIn2S4 composite photocatalyst with enhanced photocatalytic oxidation of NO under visible light. Journal of Materials Science, 2017, 52, 11453-11466.	3.7	31
38	Selective catalytic reduction of NO with NH3 over V2O5 supported on TiO2 and Al2O3: A comparative study. Journal of Molecular Structure, 2015, 1098, 289-297.	3.6	30
39	Ehanced catalytic ozonation of NO over black-TiO2 catalyst under inadequate ozone (O3/NO molar) Tj ETQq1 1	0.784314 5.6	rgBT /Overic
40	Z-scheme Caln ₂ S ₄ /Ag ₃ PO ₄ nanocomposite with superior photocatalytic NO removal performance: fabrication, characterization and mechanistic study. New Journal of Chemistry, 2018, 42, 318-326.	2.8	29
41	Facile synthesis of the Z-scheme graphite-like carbon nitride/silver/silver phosphate nanocomposite for photocatalytic oxidative removal of nitric oxides under visible light. Journal of Colloid and Interface Science, 2021, 588, 110-121.	9.4	29
42	Ni and Zn co-substituted Co(CO3)0.5OH self-assembled flowers array for asymmetric supercapacitors. Journal of Colloid and Interface Science, 2020, 573, 299-306.	9.4	28
43	Construction of octahedral BiFeWOx encapsulated in hierarchical In2S3 core@shell heterostructure for visible-light-driven CO2 reduction. Journal of CO2 Utilization, 2019, 29, 156-162.	6.8	27
44	Active sites adjustable phosphorus promoted CeO2/TiO2 catalysts for selective catalytic reduction of NO by NH3. Chemical Engineering Journal, 2021, 409, 128242.	12.7	27
45	Sodium doped flaky carbon nitride with nitrogen defects for enhanced photoreduction carbon dioxide activity. Journal of Colloid and Interface Science, 2021, 603, 210-219.	9.4	26
46	Effect of synergy between oxygen vacancies and graphene oxide on performance of TiO2 for photocatalytic NO removal under visible light. Separation and Purification Technology, 2021, 276, 119362.	7.9	26
47	Ferrous-based electrolyte for simultaneous NO absorption and electroreduction to NH3 using Au/rGO electrode. Journal of Hazardous Materials, 2022, 430, 128451.	12.4	26
48	Effect of adsorption properties of phosphorus-doped TiO2 nanotubes on photocatalytic NO removal. Journal of Colloid and Interface Science, 2019, 553, 647-654.	9.4	24
49	Insight into the combined catalytic removal properties of Pd modification V/TiO2 catalysts for the nitrogen oxides and benzene by: An experiment and DFT study. Applied Surface Science, 2020, 527, 146787.	6.1	24
50	Mechanism study on TiO2 inducing O2- and O H radicals in O3/H2O2 system for high-efficiency NO oxidation. Journal of Hazardous Materials, 2020, 399, 123033.	12.4	24
51	The effects of calcination atmosphere on the catalytic performance of Ce-doped TiO ₂ catalysts for selective catalytic reduction of NO with NH ₃ . RSC Advances, 2017, 7, 23348-23354.	3.6	23
52	Effect of rutile phase on V 2 O 5 supported over TiO 2 mixed phase for the selective catalytic reduction of NO with NH 3. Applied Surface Science, 2014, 314, 112-118.	6.1	22
53	Facile fabrication of oxygen and carbon co-doped carbon nitride nanosheets for efficient visible light photocatalytic H ₂ evolution and CO ₂ reduction. Dalton Transactions, 2019, 48, 12070-12079.	3.3	21
54	Photocatalytic oxidation of NO over TiO2-Graphene catalyst by UV/H2O2 process and enhanced mechanism analysis. Journal of Molecular Catalysis A, 2016, 423, 339-346.	4.8	20

#	Article	IF	CITATIONS
55	Novel 3D hierarchical bifunctional NiTiO3 nanoflower for superior visible light photoreduction performance of CO2 to CH4 and high lithium storage performance. Energy, 2019, 169, 580-586.	8.8	20
56	Promotional Effect of S Doping on V ₂ O ₅ –WO ₃ /TiO ₂ Catalysts for Low-Temperature NO <i>_x</i> Reduction with NH ₃ . Industrial & Engineering Chemistry Research, 2020, 59, 15478-15488.	3.7	20
57	Photocatalytic removal of NO from coal-fired flue gas by H2O2/UV reaction over TiS catalyst. Journal of Alloys and Compounds, 2017, 691, 1005-1017.	5.5	19
58	Effect of fluoride doping for catalytic ozonation of low-temperature denitrification over cerium–titanium catalysts. Journal of Alloys and Compounds, 2016, 665, 411-417.	5.5	18
59	Tailoring shape and phase formation: Rational synthesis of single-phase BiFeWOx nanooctahedra and phase separated Bi2WO6-Fe2WO6 microflower heterojunctions and visible light photocatalytic performances. Chemical Engineering Journal, 2018, 351, 295-303.	12.7	18
60	Photo-induced strong active component-support interaction enhancing NOx removal performance of CeO2/TiO2. Applied Surface Science, 2019, 476, 834-839.	6.1	18
61	Partial substitution of magnesium in lanthanum manganite perovskite for nitric oxide oxidation: The effect of substitution sites. Journal of Colloid and Interface Science, 2020, 580, 49-55.	9.4	18
62	Promoting NH3-SCR denitration via CO oxidation over CuO promoted V2O5-WO3/TiO2 catalysts under oxygen-rich conditions. Fuel, 2022, 323, 124357.	6.4	18
63	Highly efficient simulated solar-light photocatalytic oxidation of gaseous NO with porous carbon nitride from copolymerization with thymine and mechanistic analysis. RSC Advances, 2016, 6, 101208-101215.	3.6	17
64	Facial synthesis of sheet-like carbon nitride from preorganized hydrogen bonded supramolecular precursors and its high efficient photocatalytic oxidation of gas-phase NO. Journal of Photochemistry and Photobiology A: Chemistry, 2017, 340, 136-145.	3.9	17
65	The utilization of dye wastewater in enhancing catalytic activity of CeO2-TiO2 mixed oxide catalyst for NO reduction and dichloromethane oxidation. Chemosphere, 2019, 235, 1146-1153.	8.2	17
66	Reduced TiO2 inducing highly active V2O5 species for selective catalytic reduction of NO by NH3. Chemical Physics Letters, 2020, 750, 137494.	2.6	17
67	Effect of oxygen vacancies and its quantity on photocatalytic oxidation performance of titanium dioxide for NO removal. Colloids and Surfaces A: Physicochemical and Engineering Aspects, 2021, 614, 126156.	4.7	17
68	The enhancement for SCR of NO by NH3 over the H2 or CO pretreated Ag/γ-Al2O3 catalyst. Physical Chemistry Chemical Physics, 2014, 16, 12560.	2.8	14
69	Promotional effect of surface fluorine on TiO2: Catalytic conversion of O3 and H2O2 into ·OH and ·O2â^' radicals for high-efficiency NO oxidation. Chemical Engineering Journal, 2021, 424, 130358.	12.7	14
70	Active Site of O2 and Its Improvement Mechanism over Ce-Ti Catalyst for NH3-SCR Reaction. Catalysts, 2018, 8, 336.	3.5	13
71	Facile preparation of porous carbon nitride for visible light photocatalytic reduction and oxidation applications. Journal of Materials Science, 2018, 53, 11315-11328.	3.7	13
72	Active sites assembly effect on CeO2-WO3-TiO2 catalysts for selective catalytic reduction of NO with NH3. Molecular Catalysis, 2019, 479, 110549.	2.0	13

#	Article	IF	CITATIONS
73	Insight into the effect of carrier on N2O formation over MnO2/MOx (M = Al, Si and Ti) catalysts for selective catalytic reduction (SCR) of NOx with NH3. Molecular Catalysis, 2020, 488, 110916.	2.0	13
74	Promoting effect of Pd modification on the M/TiO2 (MÂ=ÂV, Ce, Mn) catalyst for catalytic oxidation of dichloromethane (DCM). Chemical Engineering Science, 2021, 234, 116405.	3.8	13
75	Study on the synergistic oxidation of sulfite solution by ozone and oxygen: Kinetics and mechanism. Chemical Engineering Science, 2021, 242, 116745.	3.8	13
76	Kinetics of Sulfite Oxidation in the Simultaneous Desulfurization and Denitrification of the Oxidationâ€Absorption Process. Chemical Engineering and Technology, 2015, 38, 797-803.	1.5	11
77	Hydrothermal Synthesis of Novel Uniform Nanooctahedral Bi ₃ (FeO ₄)(WO ₄) ₂ Solid Oxide and Visible-Light Photocatalytic Performance. Industrial & Engineering Chemistry Research, 2016, 55, 12539-12546.	3.7	11
78	CrO assembled at the oxygen vacancies on black-TiO2 for NO oxidation. Molecular Catalysis, 2019, 473, 110393.	2.0	11
79	Using excess O3 to facilitate the NO2 absorption in a sulfite solution: Process conditions and mechanism. Fuel Processing Technology, 2020, 206, 106457.	7.2	11
80	Effect of fluorine additives on the performance of amorphous Ce-Ti catalyst and its promotional progress on ozone for NO X (x = 1, 2) removal at low temperature. Journal of Fluorine Chemistry, 2016, 191, 120-128.	1.7	10
81	Catalytic ozonation of NO into HNO3 with low concentration ozone over MnO -CeO2/TiO2: Two-phase synergistic effect of TiO2. Molecular Catalysis, 2020, 493, 111095.	2.0	10
82	Revealing active species of CePO4 catalyst for selective catalytic reduction of NO with NH3. Journal of Rare Earths, 2022, 40, 1232-1237.	4.8	10
83	Formation of flaky carbon nitride and beta-Indium sulfide heterojunction with efficient separation of charge carriers for enhanced photocatalytic carbon dioxide reduction. Journal of Colloid and Interface Science, 2022, 611, 71-81.	9.4	10
84	Selective denitrification of flue gas by O3 and ethanol mixtures in a duct: Investigation of processes and mechanisms. Journal of Hazardous Materials, 2016, 311, 218-229.	12.4	9
85	Experimental study on reaction characteristics of NO in (NH4)2SO3 solution. Journal of Industrial and Engineering Chemistry, 2018, 65, 380-386.	5.8	9
86	Sulfur-doping promoting peroxone reaction over TiO2 for highly effective NO oxidation at low temperature: Experimental and DFT studies. Chemical Engineering Journal, 2022, 429, 132475.	12.7	9
87	Tailorable boron-doped carbon nanotubes as high-efficiency counter electrodes for quantum dot sensitized solar cells. Catalysis Science and Technology, 2021, 11, 2745-2752.	4.1	9
88	Cluster molecular modeling of strong interaction for F-doped V2O5–WO3/TiO2 supported catalyst. Journal of Fluorine Chemistry, 2013, 153, 26-32.	1.7	8
89	The inhibition effect of oxygen inÂthe calcination atmosphere on the catalytic performance of MnOx–CeO2 catalysts for NO oxidation. Reaction Kinetics, Mechanisms and Catalysis, 2017, 122, 593-604.	1.7	8
90	Deep insight into the catalytic removal mechanism of a multi-active center catalyst for chlorobenzene: an experiment and density functional theory study. Catalysis Science and Technology, 2020, 10, 6879-6891.	4.1	8

#	Article	IF	CITATIONS
91	Promotional effect of surface fluorine species on CeO2 catalyst for toluene oxidation. Molecular Catalysis, 2021, 512, 111771.	2.0	8
92	The effect of preparation method on oxygen activation over Pt/TiO2 catalysts for toluene total oxidation. Chemical Physics Letters, 2019, 730, 95-99.	2.6	7
93	Highly efficient K-doped Mn–Ce catalysts with strong K–Mn–Ce interaction for toluene oxidation. Journal of Rare Earths, 2023, 41, 374-380.	4.8	7
94	Efficient Inhibition of N ₂ O during NO Absorption Process Using a CuO and (NH ₄) ₂ SO ₃ Mixed Solution. Industrial & Engineering Chemistry Research, 2018, 57, 13010-13018.	3.7	6
95	V2O5-(NH4)2V6O16·1.5H2O composite catalysts as novel platforms for high-efficiency catalytic ozonation of NO under low temperature. Journal of Physics and Chemistry of Solids, 2021, 155, 110112.	4.0	6
96	SO ₂ Poisoning Mechanism of the Multi-active Center Catalyst for Chlorobenzene and NO _{<i>x</i>} Synergistic Degradation at Dry and Humid Environments. Environmental Science & Technology, 2021, 55, 13186-13197.	10.0	6
97	Synergistic effect of F and triggered oxygen vacancies over F-TiO2 on enhancing NO ozonation. Journal of Environmental Sciences, 2023, 125, 319-331.	6.1	6
98	Inhibition effect of naphthalene on V2O5-WO3/TiO2 catalysts for low-temperature NH3-SCR of NO. Fuel, 2022, 322, 124157.	6.4	6
99	Highly-dispersed CoS2/N-doped carbon nanoparticles anchored on RGO skeleton as a hierarchical composite counter electrode for quantum dot sensitized solar cells. Chemical Engineering Journal, 2022, 430, 132732.	12.7	5
100	Insight Into the CuOx Interacts with Oxygen Vacancies on the Surface of Black-TiO2 for NO Oxidation. Catalysis Letters, 2022, 152, 2869-2879.	2.6	5
101	The effect of polyethylene glycol modification on CrO /TiO2 catalysts for NO oxidation. Colloids and Surfaces A: Physicochemical and Engineering Aspects, 2019, 578, 123588.	4.7	4
102	CrOx Anchored on the Black-TiO2 Surface via Organic Carboxylic Acid Ligand and Its Catalysis in Oxidation of NO. Catalysis Letters, 2021, 151, 1755-1765.	2.6	4
103	Mechanism and Kinetic Study of Cyclodextrin Use to Facilitate NO ₂ Absorption in Sulfite Solutions. Environmental Science & amp; Technology, 2022, 56, 7696-7706.	10.0	4
104	TiO2 with exposed {0 0 1} facets catalyzed peroxone reaction into ·O2– and ·OH radicals for low temperature NO oxidation. Fuel, 2022, 314, 122748.	6.4	3
105	New insight on N2O formation over MnOx/TiO2 catalysts for selective catalytic reduction of NOx with NH3. Molecular Catalysis, 2022, 525, 112356.	2.0	3
106	Study on the Dephenolization of wastewater of coal chemical industry. Proceedings of the Mongolian Academy of Sciences, 0, , 36-44.	0.0	0
107	The mechanism of Ce-MCM-41 catalyzed peroxone reaction into •OH and •O2â^' radicals for enhanced NO oxidation. Molecular Catalysis, 2022, 518, 112110.	2.0	0